

Isolation and modification of nano-scale cellulose from organosolv-treated birch through the synergistic activity of LPMO and endoglucanases

Madhu Nair Muraleedharan^a, Anthi Karnaouri^{a,*}, Maria Piatkova^b, Maria-Ximena Ruiz-Caldas^b, Leonidas Matsakas^a, Bing Liu^c, Ulrika Rova^a, Paul Christakopoulos^a, Aji P. Mathew^{b,*}

^a Biochemical Process Engineering, Chemical Engineering, Department of Civil, Environmental and Natural Resources Engineering, Luleå University of Technology, 97187 Luleå, Sweden

^b Department of Materials and Environmental Chemistry, Stockholm University, 10691 Stockholm, Sweden

^c Department of Molecular Sciences, Swedish University of Agricultural Sciences, Uppsala, Sweden

ARTICLE INFO

Article history:

Received 28 February 2021

Received in revised form 18 April 2021

Accepted 22 April 2021

Available online 24 April 2021

Keywords:

Nanocellulose

LPMO biocatalysis

Post-treatment modification/functionalization

ABSTRACT

Nanocellulose isolation from lignocellulose is a tedious and expensive process with high energy and harsh chemical requirements, primarily due to the recalcitrance of the substrate, which otherwise would have been cost-effective due to its abundance. Replacing the chemical steps with biocatalytic processes offers opportunities to solve this bottleneck to a certain extent due to the enzymes substrate specificity and mild reaction chemistry. In this work, we demonstrate the isolation of sulphate-free nanocellulose from organosolv pretreated birch biomass using different glycosyl-hydrolases, along with accessory oxidative enzymes including a lytic polysaccharide monoxygenase (LPMO). The suggested process produced colloidal nanocellulose suspensions (ζ -potential -19.4 mV) with particles of 7–20 nm diameter, high carboxylate content and improved thermostability ($T_0 = 301$ °C, $T_{max} = 337$ °C). Nanocelluloses were subjected to post-modification using LPMOs of different regioselectivity. The sample from chemical route was the least favorable for LPMO to enhance the carboxylate content, while that from the C1-specific LPMO treatment showed the highest increase in carboxylate content.

© 2021 The Authors. Published by Elsevier B.V. This is an open access article under the CC BY license (<http://creativecommons.org/licenses/by/4.0/>).

1. Introduction

Nanocellulose is considered as one of the key value added products in the emerging market of biodegradable, green polymers. Due to its distinctive physical and chemical properties, this high-value product exhibits a wide repertoire of applications, ranging from polymer composites to super-capacitors, as reviewed by Trache et al. [1]. Nanocellulose can be described as cellulose particles with at least one of their dimensions, often diameter, in nanometric scale (below 100 nm) [2,3]. It can be produced from almost any cellulose-rich material found in nature, such as tunicates and plant-based lignocellulosic biomass [4,5]. The latter has attracted particular interest for nanocellulose production due to its high availability and low cost compared to other sources [6].

The physical and chemical properties of nanocellulose such as dimensions, aspect ratios and surface charges as well as energy consumption of extraction are dependent on the source of cellulose and the

process of extraction [7,8]. While an enzymatic and/or mechanical disintegration results in cellulose nanofibres (CNFs) [9], a much harsher treatment with concentrated mineral acids, such as sulphuric acid, would enable to obtain highly crystalline cellulose nanocrystals (CNCs) [8,10]. In cellulose nanofibers, both amorphous and crystalline domains exist whereas nanocrystals can be isolated after removing the amorphous cellulose domains through strong mineral acid treatment [11]. Additionally, defibrillation can be facilitated by modifying the surface charge of cellulose by using TEMPO (2,2,6,6-tetramethylpiperidine-1-oxyl radical)-mediated oxidation [12] or carboxymethylation [13]; although these chemical treatments drastically drop the high-energy requirements for nanocellulose isolation, they meet several limitations due to high environmental impacts. In addition, the sulphated nanocellulose produced from the employment of sulphuric acid, has several drawbacks, such as lower thermal stability and potential cytotoxicity that dent its use in polymer and medical applications, respectively [14,15]. Therefore, alternative approaches employing milder and greener techniques are being explored [16]. Among these, biocatalysis is an environmentally friendly process of utmost importance, due to its targeted and substrate-specific activity, selectivity, mild and non-toxic chemistry. Besides, unlike in case of

* Corresponding authors.

E-mail addresses: anthi.karnaouri@tu.se (A. Karnaouri), aji.mathew@mmk.su.se (A.P. Mathew).

chemical hydrolysis, the sugar-rich side stream that is co-produced with nanocellulose upon enzymatic treatment is devoid of toxic, inhibitory components and can be directly converted to many value added products through microbial fermentation [6,17]. All the above mentioned render biocatalysis a key factor for integrating production of nanocellulose as a novel industrial product of lignocellulose biorefineries, while ensuring process efficiency and sustainability [6].

Cellulases constitute a class of enzymes with exceptional properties that are gradually replacing and reducing the need for harsh chemicals in different industrial applications, including textiles, detergents, cosmetics, food, animal feed, agriculture [18] and, most recently CNCs and CNFs [19,20]. Among them, enzymes with endo-activity, namely endoglucanases, are the most exploited enzymes for the production of nanocellulose due to their potential to remove the less ordered amorphous regions from cellulose fibers, leaving intact the more organized, crystalline areas, thus facilitating the nanocellulose isolation without altering the cellulose surface chemistry [19–21]. There are recent studies demonstrating that the incorporation of a cellulase-catalyzed treatment step in the nanocellulose isolation process led to better CNFs yield and quality and reduced the use of acid in case of CNCs production [22,23]. Moreover, enzymes have been employed to assist TEMPO (2,2,6,6-tetramethylpiperidine-1-oxyl radical) - mediated oxidation, which increases the carboxylate group content of cellulose and therefore facilitates the isolation of nanocellulose [24]; however, the use of TEMPO compromise the thermostability of the product [25]. Moreover, most of these works have been conducted with commercial cellulase mixtures, which exhibit a broad activity for cellulose hydrolysis and are not specific for nanocellulose production; their primary role is to liquefy the substrate into soluble sugars, thus their use may affect the yield of nanocellulose obtained. Limited attempts have been made to isolate nanocellulose void of acid hydrolysis [25,26] or without the use of cellulase mixtures [25,27].

Apart from cellulolytic enzymes, other accessory activities, such as laccases that react with the lignin fraction of lignocellulosic biomass [28], and xylanases [27,29] that remove hemicelluloses, are known players for the isolation of nanocrystalline cellulose, in the form of either fibers or crystals. Another class of carbohydrate-acting enzymes involves lytic polysaccharide monoxygenases (LPMOs) that cleave cellulose by a unique oxidative reaction, in the presence of molecular oxygen or hydrogen peroxide as co-substrate, and an electron donor [30]. The boosting effect of LPMOs when acting in synergy with cellulases for the liquefaction of cellulosic substrates is well known [31,32], while they are currently gaining increasing attention due to their potential implication in nanocellulose production [27,33,34]. The ability of a particular group of LPMOs that cleave the cellulose chain by oxidizing C1 carbon to introduce carboxylate groups to the substrate has been related to disintegration of cellulose fibrils and enhancement of nanocellulose production [6,26,27,34,35].

In the present study, we attempted to isolate nano-scale cellulose from forest biomass by using different monoenzymes with targeted action, and the outcome of the enzymatic route was compared with the traditionally used chemical process. The effects of endoglucanase, xylanase, laccase and C1-specific LPMO activity on the yield and the properties of the final product were evaluated. The aim was to assess the potential of biocatalysis to progressively replace the use of chemicals to remove hemicellulose, lignin, and amorphous regions of cellulose and introduce carboxylate groups on cellulose surface, thus boosting the nanocellulose production from organosolv pretreated birch. Moreover, post-modification of isolated samples was evaluated using two LPMOs with different regioselectivity, namely the C1-specific PclLPMO9D from *Phanerochaete chrysosporium* [36] and the mixed C1/C4-specific MtlLPMO9H from *Thermothelomyces thermophila* (previously known as *Myceliophthora thermophila*) [31] in order to assess their individual effect.

2. Materials and methods

2.1. Organosolv pretreatment of wood biomass

Organosolv (without acid) pretreated birch was used as the feedstock for the process. Bark-free birch woodchips (*Betula pendula* L.) were used as raw material during the current work. Prior to organosolv fractionation, woodchips were milled through a 1-mm screen in a Retsch SM 300 knife mill (Retsch GmbH, Haan, Germany). Organosolv fractionation of milled woodchips took place in 2.5-L metallic cylinders that were placed in an air-heated multidigester as previously described [37]. The metallic vessels were filled with 110 g of dried woodchips and 1.1 L of a 50% v/v ethanol to water solution. Fractionation took place at 183 °C for 1 h under constant mild mixing by rotation. After the treatment time elapsed, the vessels were allowed to cool down to room temperature under constant mixing. After that, the pretreated solids were recovered from the liquor by vacuum filtration, washed with the same solution used during fractionation, air dried and stored until further use. The liquor was used to isolate lignin and hemicellulose, which were not used in the current work. The compositional analysis of the pretreated solids was determined following the NREL protocols [38] and the results expressed in dry basis were (wt%): cellulose, 57.1; hemicellulose, 19.3; lignin, 13.2.

2.2. Heterologous cloning of MtlLPMO9H in pGAPZαC vector

M. thermophila MtlLPMO9H [31] was expressed and produced in *Pichia pastoris* X33 strain. The gene XP_003661787 encoding the predicted amino acid sequence was obtained from <https://mycocosm.jgi.doe.gov/mycocosm/home> (MYCTH_46583) and was inserted as a synthetic gene in pGAPZαC vector (Invitrogen, San Diego, CA), downstream of the GAP (glyceraldehyde-3-phosphate dehydrogenase) promoter. Due to the presence of N-terminal active site of the LPMO, the native signal peptide of the enzyme was chosen, and the restriction sites *Bst*BI and *Xba*I were selected for the gene insert to remove the α-factor secretion signal of the vector. Before transforming the plasmid into the *P. pastoris*, the recombinant pGAPZαC- MtlLPMO9H was amplified in *One Shot*TM TOP10 chemically competent cells (InvitrogenTM) according to the product guidelines and the transformants were selected by plating on Luria-Bertani (LB) agar plates with 25 µg/ml ZeocinTM. Single colony from a re-streaked fresh plate was chosen to inoculate 5 ml of LB medium with 25 µg/ml ZeocinTM and incubated for 12 h, at 37 °C and 200 rpm agitation. Bacterial culture was harvested and the amplified plasmid DNA was purified using GeneJET Plasmid Miniprep Kit (Thermo ScientificTM). Purified plasmid DNA was linearized using FastDigestTM BglIII restriction enzyme (Thermo ScientificTM) and transformed into *P. pastoris* following the protocols of the *Pichia* expression vectors for constitutive expression and purification of recombinant proteins manual (Catalog nos. V200–20 and V205–20). Transformants with high cassette expression were selected by streaking on yeast-peptone medium with 2% glucose (YPD) agar plates with ZeocinTM concentrations from 100 µg/ml, 200 µg/ml, 300 µg/ml. Single colonies grown in 300 µg/ml were picked to re-streak on fresh YPD plates with 300 µg/ml ZeocinTM and stored in 4 °C.

2.3. Production and purification of MtlLPMO9H and PclLPMO9D

The recombinant *P. pastoris*-MtlLPMO9H and *P. pastoris*-PclLPMO9D strains were cultivated in 3 L bioreactor, following the *Pichia* fermentation process guidelines (Version B 053002). Cells were first grown at 30 °C in 100 ml YPD medium, in 1 L shake flasks, buffered with 100 mM phosphate buffer at a pH of 6.0 in a shaking incubator (180 rpm) until the cell density reached an OD₆₀₀ of 3. Cells were aseptically harvested by centrifugation at 2500 xg for 15 min. Pellets were resuspended to 1 L YPD to reach a starting OD₆₀₀ of 1, in a 3 L bioreactor (Applikon Biotechnology), buffered with 100 mM phosphate buffer pH 6.0 and controlled by 20% ammonia base solution. Temperature was set to 30 °C

and dissolved oxygen (DO) as 20%, controlled by a constant airflow and automatic agitation varying from 450 to 850 rpm. Cells were grown for 5–6 days and glucose was pumped from a 50% (w/v) stock using the integrated acid-pump of the bioreactor taking the advantage of the ‘feedback mechanism’ that pH level raises when the carbon source runs out. Purification of *MtLPMO9H* was performed with immobilized metal affinity chromatography (IMAC) using a cobalt ion charged resin as previously described [39]. In case of *PcLPMO9D*, the enzyme was purified with hydrophobic interaction chromatography (HIC), after precipitation with ammonium sulphate, following an already developed protocol [36].

2.4. Isolation of cellulose nanocrystals

2.4.1. Disruption and removal of the lignin-hemicellulose matrix

The organosolv pretreated biomass was used as a starting material for the isolation of nano-scale cellulose. For the chemical route, as depicted in Fig. 1A (Route 1), the substrate was first subjected to alkaline hydrolysis and bleaching treatment. Alkali treatment step involved boiling of the biomass with 5 wt% KOH under stirring for 6 h to swell the fibers, facilitate the infiltration of the bleaching solution and lead to the removal of hemicellulose. The final suspension was extensively washed with distilled H₂O and was subsequently bleached upon

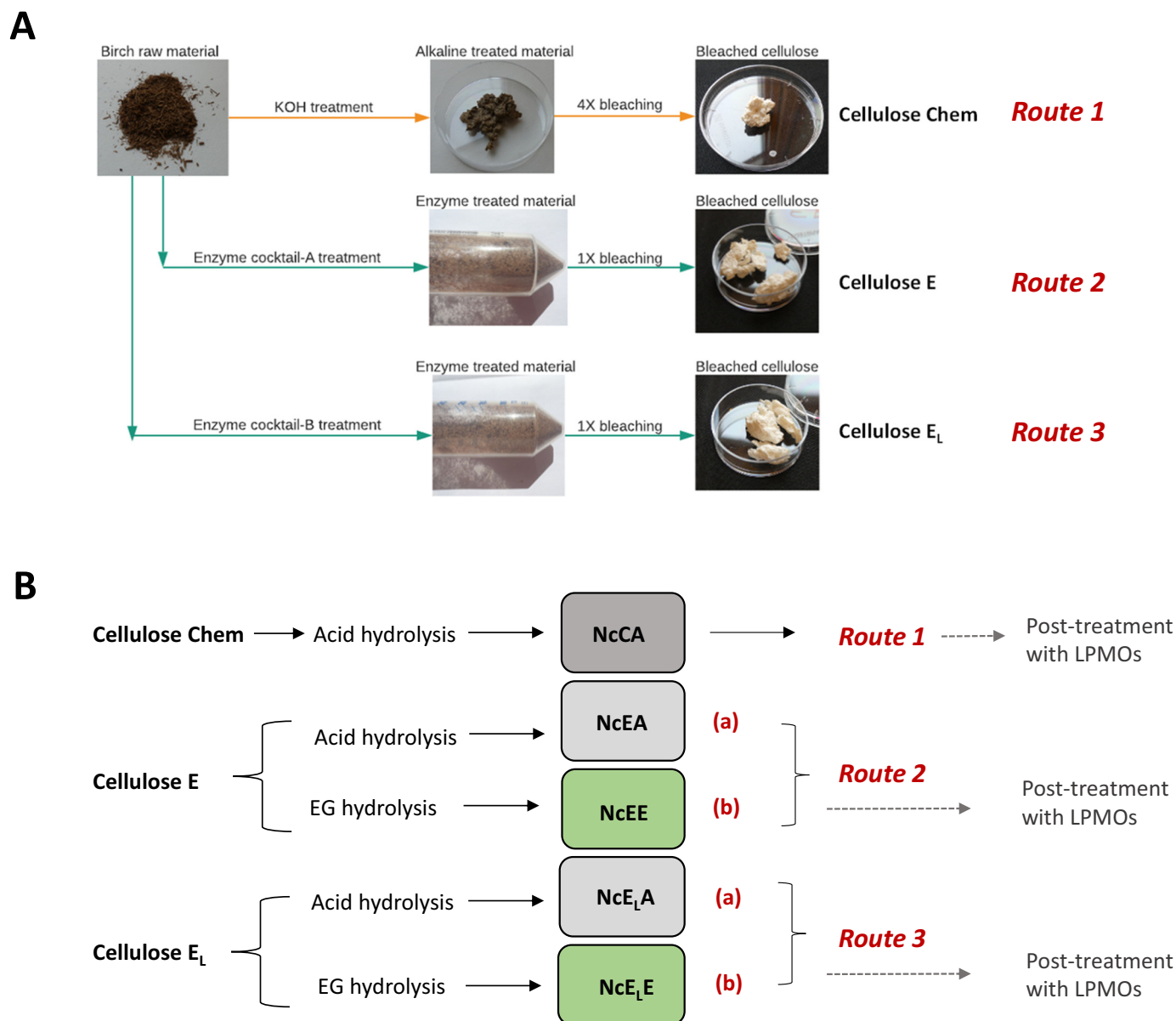


Fig. 1. (A) Removal of hemicellulose and lignin by chemical and enzymatic processes. *Route 1* involves alkaline treatment of organosolv pretreated birch with KOH solution followed by four bleaching steps, yielding bleached Cellulose Chem. In *Route 2* and *3*, alkaline KOH treatment is replaced by enzymatic treatment with two different cocktails, followed by one single bleaching step, yielding bleached Cellulose E and Cellulose E_L respectively. (B) Schematic representation of the three different processes followed for the production of nano-scale cellulose from organosolv pretreated birch biomass. *Route 1* followed the traditional chemical isolation pathway using sulphuric acid hydrolysis of Cellulose Chem sample for the removal of amorphous cellulose regions. In case of *Route 2* and *3*, bleached Cellulose E and Cellulose E_L were subjected to either acid hydrolysis (*Route 2a* and *3a*) or treatment with endoglucanases (*Route 2b* and *3b*) respectively. The produced samples are NcCA: cellulose nanocrystals from chemical pathway (alkaline hydrolysis and 4 bleaching steps), hydrolyzed with acid. NcEA: cellulose nanocrystals from enzymatic pretreatment with cocktail A and one bleaching step, hydrolyzed with acid. NcEE: nano-scale cellulose from enzymatic pretreatment with cocktail A and one bleaching step, hydrolyzed with endoglucanase mixture. NcE_LA: cellulose nanocrystals from enzymatic pretreatment with cocktail B and one bleaching step, hydrolyzed with acid. NcE_LE: nano-scale cellulose from enzymatic pretreatment with cocktail B and one bleaching step, hydrolyzed with endoglucanase mixture.

addition of 0.19 M sodium chlorite in 0.3 M sodium acetate buffer, at 80 °C for 6 h, under agitation. The samples were extensively washed with distilled H₂O and the final product was centrifuged for 15 min at 10000 rpm; the precipitate was collected and resuspended in distilled H₂O. The bleaching step was repeated 4 times.

Along with the traditional acid-catalyzed chemical process, two separate enzymatic pathways were designed using different combinations of hydrolases and accessory enzymes, as depicted in Fig. 1B (*Route 2 and 3*). Enzymatic cocktail A contained a mixture of two endoglucanases, one belonging to glycoside hydrolase family 5 (EG5) from *Talaromyces emersonii* (Megazyme) and one belonging to glycoside hydrolase family 7 (EG7) from *Trichoderma longibrachiatum* (Megazyme), together with xylanase (ACCELLERASE® XY, Genencor) and laccase from the fungus *Pycnoporus cinnabarinus* (kindly provided by Beldem, Belgium). Enzymatic cocktail B comprised of the same mixture as cocktail A, in addition to the C1-specific P_cLPMO9D [37]. All enzymes were added at a final concentration of 5 mg/g substrate in the reaction mixture. Reactions took place at 50 °C, 1000 rpm agitation, in 50 mM sodium acetate buffer pH 5.0, in the presence of 1 mM ascorbic acid for 24 h. Reaction was stopped by heating the mixture at 95 °C for 15 min, followed by extensive washing with de-ionized water until the pH stabilized at around 7.0. After enzymatic treatment, one single bleaching step followed in order to complete refining and attain cellulose fraction for further processing.

2.4.2. Removal of cellulose amorphous regions

For the removal of cellulose amorphous regions from the bleached samples, two approaches were followed, including acid hydrolysis and enzymatic treatment with endoglucanases, as depicted in Fig. 1B. In case of the chemical process (*Route 1*), cellulose nanocrystals were prepared by following a modified version of the process reported by Bondeson et al. [10]. The aqueous suspension of bleached biomass was mixed with H₂SO₄ to reach a final acid/H₂O concentration of 61% wt. and it was incubated at 70 °C under vigorous stirring for 20 min. In case of *Route 2a and 3a* (Fig. 1B), the acid concentration was reduced to 54–55% wt. and it was incubated at 70 °C under vigorous stirring for 15 min. In all cases, the hydrolysis was quenched by adding excess of distilled water and was allowed to cool down to room temperature. The suspension was successively centrifuged at 5000 rpm for 15 min to concentrate the cellulose nanocrystals and to remove the excess of aqueous acid. The isolated nanocrystals were rinsed and dialyzed in distilled H₂O until pH 4–5 was reached. The suspension was sonicated using a Qsonica Q500, 500-watt Sonicator at 75% output for 5 min. For the enzymatic treatment with endoglucanases (*Route 2b and 3b*, Fig. 1B), EG5 and EG7 were used instead of acid, at an enzyme loading of 10 mg of each enzyme/g of substrate. The isolated nano-scale cellulose was characterised as described below.

2.5. Enzymatic LPMO post-treatment of nanocellulose

LPMO post-treatment of isolated nano-scale cellulose was conducted with two different LPMOs, namely the C1-specific P_cLPMO9D [36] and the mixed C1/C4-specific M_tLPMO9H [31]. The reaction took place at an enzyme loading of 10 mg/g substrate, at 50 °C, 1000 rpm agitation, in 50 mM sodium acetate buffer pH 5.0, in the presence of 1 mM ascorbic acid and incubated for 12 h. In order to terminate the reaction, the mixture was heated at 95 °C for 15 min, followed by extensive washing with de-ionized water until the pH stabilized at around 7.0. The soluble sugars released after the post-treatment with LPMOs were detected with HPAEC-PAD (high-performance anion-exchange chromatography with pulsed amperometric detection) as previously described [31] and the oxidized and neutral sugars were assessed based on previous data [40]. The surface groups were identified with XPS, as described below.

2.6. Characterization of nanocellulose morphology and surface chemistry

2.6.1. Atomic force microscopy (AFM)

Topographical surface images were captured using an atomic force microscope (AFM, Veeco Multimode V, USA) operating in tapping mode and of height, amplitude, and phase images were recorded. For analysis, a droplet of diluted suspension of the sample was deposited on freshly cleaved mica sheet and allowed to dry. The diameter measurements were performed using the Nanoscope V software from the height images.

2.6.2. Scanning electron microscopy (SEM)

Scanning electron microscopy (SEM) of the cellulose fibers was studied using a TM3000 microscope (Hitachi) with accelerating voltage 5 kV. The samples were deposited on carbon tape and were sputter coated with gold prior to imaging.

2.6.3. Zeta-potential analysis

Zeta-potential was measured assuming Smoluchowski behavior with a Zetasizer Nano ZS (Malvern Instruments) equipped with a universal dip cell. Dispersions of ≤0.01 wt% in 10 mM NaCl were measured 10 times with each measurement composed of 12 runs. The error corresponds to the standard deviation.

2.6.4. X-ray photoelectron spectroscopy (XPS)

The surface groups of CNCs were identified and quantified via XPS. The analyses were performed with an Axis Ultra DLD electron spectrometer (Kratos Analytical Ltd., U.K.) using a monochromatized Al K α radiation source operating at 150 W and an energy of 20 eV for individual photoelectron lines. The high-resolution spectra were fitted using a series of Gaussian peaks.

2.6.5. Thermogravimetric analysis (TGA)

The thermal properties of the samples were tested by a thermogravimetric analyzer (TA Instruments Discovery) under air atmosphere at a flow rate of 20 ml/min. Samples weighing >1 mg were analyzed at a constant heating rate of 10 °C/min from ambient temperature to 600 °C.

3. Results and discussion

3.1. Isolation of nano-scale cellulose

For the isolation of nano-scale cellulose from organosolv pretreated birch, disruption and removal of the lignin-hemicellulose matrix took place through alkaline hydrolysis, as depicted in Fig. 1A, in order to obtain a cellulose-rich pulp, which was then subjected to hydrolysis for the removal of amorphous regions leaving behind the highly crystalline areas. Three different processes were evaluated. *Route 1* followed the traditional chemical isolation pathway using sulphuric acid hydrolysis for the removal of amorphous cellulose regions. Along with the traditional acid-catalyzed chemical process, two separate enzymatic pathways were designed using two enzymatic cocktails, A and B, with different combinations of hydrolases and accessory enzymes, as described in Materials and Methods section. The fractions after the enzymatic treatment with either cocktail A or B (*Routes 2 and 3*, respectively), were directly subjected to one single bleaching step, without any alkaline treatment. In the next step, the bleached biomass was subjected to either acid hydrolysis (*Route 2a and 3a*) or treatment with endoglucanases (*Route 2b and 3b*).

In order to evaluate the effect of enzymatic pretreatment in the morphology and structure properties of the biomass, the organosolv treated samples, either without (Fraction 1-*Route 1*) or after enzymatic treatment with cocktail A and B (Fraction 2-*Route 2* and Fraction 3-*Route 3*, respectively), were studied with SEM, prior to any alkaline and/or bleaching step. The results (Supplementary material, Fig. S1) showed that there are morphological differences in samples after the enzymatic

treatment. The fibers in Fraction 1 exhibit an uneven, hairy surface, while the enzyme-pretreated fractions (Fraction 2 and 3) showed a smoother texture, due to the removal of amorphous regions and polishing after the activity of enzymes. However, no significant differences could be observed between the two enzyme-treated fractions.

A summary of the overall process for the production of different nano-scale celluloses is presented in Fig. 1B, showing the samples that were isolated from different routes: (i) NcCA was obtained from chemical pathway (alkaline hydrolysis and 4 bleaching steps) and was hydrolyzed with acid. (ii) NcEA was obtained from enzymatic pretreatment with cocktail A and one bleaching step, and was hydrolyzed with acid. (iii) NcEE was obtained from enzymatic pretreatment with cocktail A and one bleaching step, and was hydrolyzed with endoglucanase mixture. (iv) NcE_LA was obtained from enzymatic pretreatment with cocktail B and one bleaching step, and was hydrolyzed with acid. (v) NcE_LE

was obtained from enzymatic pretreatment with cocktail B and one bleaching step, and was hydrolyzed with endoglucanase mixture.

The results show that the enzymatic pretreatments could reduce the bleaching process down to 4 times lower than the chemical pathway. The use of endoglucanase-assisted treatment instead of acid hydrolysis to remove amorphous regions seemed feasible and enabled the production of sulphur-free nanocellulose. Although the use of a cellulase cocktail, such as Celluclast and Cellic® CTEC2, would increase the pretreatment efficiency, it has certain drawbacks as well. These enzyme mixtures are non-specific and may not be favorable for removing only the amorphous cellulose regions, leaving behind the highly crystalline nanocellulose. Moreover, the composition of these cocktails is primarily optimized for achieving maximum liquefaction of lignocellulose into soluble sugars [41], while the use of different monoenzymes allows for the optimization of hydrolysis conditions through controlled enzymatic treatment to avoid excessive liquefaction [25,42]. In the process

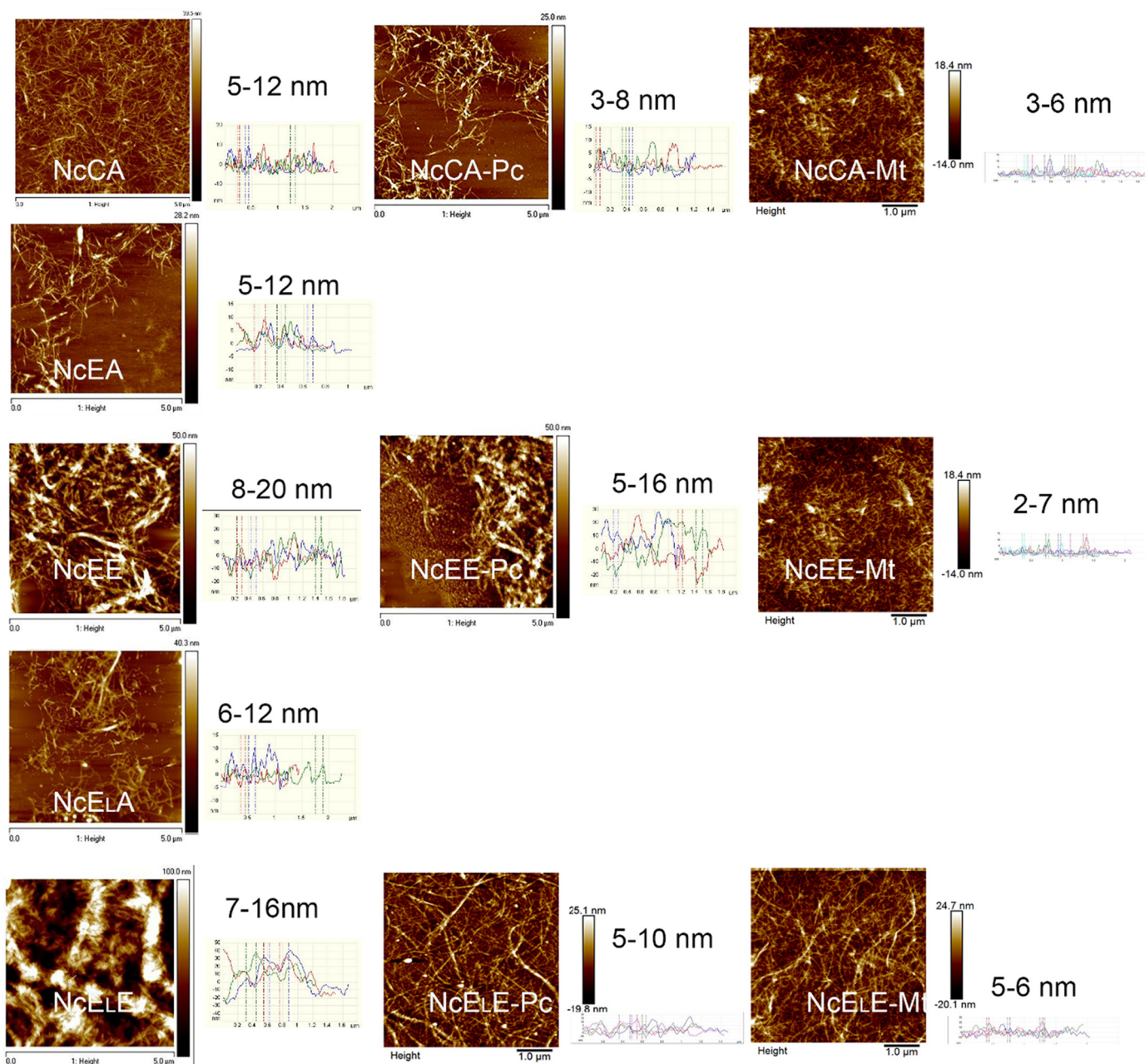


Fig. 2. AFM images and width values of isolated nanocellulose from different routes.

followed in this work, it is verified that a combination of cellulases and xylanases, together with laccases and LPMOs can be used either synergistically or individually to tailor the removal of amorphous regions towards the isolation of nanocellulose.

3.2. Morphology of isolated nanocellulose samples

The average width of the isolated nanocellulose after three different routes was identified using AFM and the results are depicted in Fig. 2. As it can be observed, there is no significant difference in the length among samples that have been treated with acid for the removal of cellulose amorphous regions (NcCA, NcEA, NcE_LA), which correspond to Routes 1, 2a and 3a. These samples represent cellulose nanocrystals (CNCs) and have the typical size, as reported in the literature. Among the strict enzyme Routes 2b and 3b, pretreatment with the enzyme cocktail B that contained LPMO in addition to hydrolytic enzymes, resulted in thinner particles of 7–16 nm diameter (NcE_LE) compared to those obtained after treatment with cocktail A that exhibited a diameter of 8–20 nm diameter (NcEE). These samples represent nano-scale cellulose of mixed elements with various diameters, comprised mainly of long interconnected cellulose fibrils (CNFs) together with, to a lesser extent, CNCs, as shown in Fig. 2. Regarding the overall structure and the diameter of the CNFs obtained from Routes 2b and 3b, they are both comparable to those from other studies employing enzymes for nanocellulose isolation. Rossi et al. obtained similar results from sugarcane bagasse (fibrils with 1.3–20 nm width) after treatment with endoglucanase, xylanase and an LPMO of AA9 family [25], while treatment with endoglucanase yielded nanocellulose of 5–7 nm width from natural bast fibers [20], corroborating that the enzymes are very efficient to produce nano-scale cellulose. Valls et al. obtained thicker elements from cotton linters after treatment with a mixture of cellulases and an AA10 LPMO [28].

The heterogeneity observed in the morphology of samples produced by the strict enzymatic routes (Routes 2b and 3b) is attributed to the activity of endoglucanases that perform a milder hydrolysis compared to sulphuric acid, targeting specifically to digest amorphous regions leaving intact the crystalline areas [43]. This mode of action results in heterogeneity and a wide range of size distribution in the final nano-scale product, which has also been reported in the work by Teixeira et al. 2015 [19]. Compared to the processes that involve the acid hydrolysis step and lead to the production of CNCs, the strict enzymatic routes provided nanoscale cellulose with properties close to CNFs. CNCs and CNFs

are two products with different properties, so the process selection for the final product depends on the relevant application that is targeted. When it comes to the production of CNCs, though coming with a high environmental cost, sulphuric acid treatment still consists the most widely used process that yields crystals with targeted qualities such as excellent colloidal dispersion and high crystallinity [8]. On the other side, in case of the enzyme-assisted treatment, the process still needs fine-tuning in order to obtain CNC-grade nanocellulose that meets the industrial-grade quality requirements, similar to that obtained through acid treatment. However, the process yields CNFs with high aspect ratio [25]. Moreover, enzymatic routes provide greener processes in isolating nanoscale cellulose and, thus, they could replace chemicals to a great extent. The highest significance of employing biocatalysis for nanocellulose isolation can be outlined within the frame of a biorefinery concept, where nanocellulose is produced as a side-product in the production of soluble fermentable sugars [6,44,45]. The above observations make clear that both chemical and enzymatic route have its own relevance, targeting at different nanocellulose products.

3.3. Analysis of surface charge, evaluation of carboxylate groups and thermal stability

Zeta-potential values at pH 7.0 were determined for all samples obtained from the three different routes as a primary indication of their net surface charge and are described in Fig. 3. The NcCA sample isolated from the chemical process (Route 1) displayed the highest absolute value of zeta-potential (−31.0 mV), indicating the strong repulsion of the negatively charged nanocrystals. Similar values of zeta-potential of LPMO-treated nano-scale cellulose have been reported in previous studies for different types of plant and tunicate biomass [5,26,34,35]. Replacement of alkaline hydrolysis with enzymatic treatment with cocktails A or B, combined with acid hydrolysis (Routes 2a and 3a) resulted in well-dispersed fibers with zeta-potential values of −25.5 mV and −24.8 mV respectively, verifying a good colloidal stability of these samples. The surface charge of these samples can be attributed mainly to the sulphate groups introduced during acid hydrolysis, as well as, in case of Route 3a, to the carboxylate groups as a result of the C1-specific LPMO activity. It has been reported that treatment with sulphuric acid leads to introduction of sulphate groups at the C6 carbon on the glucose molecule of the cellulose chain [46]. These charged groups probably cause the reduction in the zeta-potential in CNCs

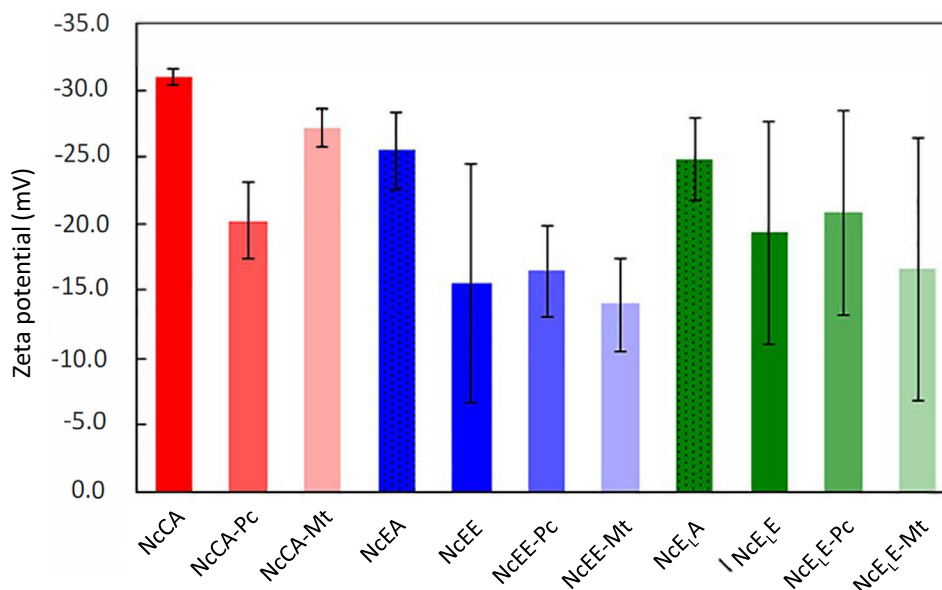


Fig. 3. Zeta-potential values for the isolated nano-scale cellulose prior and after post-treatment with different LPMOs.

Table 1

Atomic percentage (%) of carboxylate and sulphate groups of isolated nano-scale cellulose prior and after post-treatment with different LPMOs.

Sample	-COOH	-HSO ₃ -
NcCA	0.78	0.27
NcCA treated with PclPMO (NcCA-Pc)	0.74	0.12
NcCA treated with MtlPMO (NcCA-Mt)	0.66	0.16
NcEA	0.36	0.13
NcEE	0.56	–
NcEE treated with PclPMO (NcEE-Pc)	1.26	–
NcEE treated with MtlPMO (NcEE-Mt)	0.95	–
NcE ₁ A	0.51	0.18
NcE ₁ E	0.79	–
NcE ₁ E treated with PclPMO (NcE ₁ E-Pc)	1.55	–
NcE ₁ E treated with MtlPMO (NcE ₁ E-Mt)	0.6	–

isolated after acid hydrolysis. When acid hydrolysis was replaced by treatment with endoglucanases (*Routes 2b* and *3b*), the absolute value of zeta-potential was lower (−15.6 mV and −19.4 mV respectively), due to the absence of sulphate groups. As both acid and enzyme-assisted treatment are expected to remove the amorphous cellulose regions, and since the latter is not able to introduce any additional charged group, decrease of the zeta-potential absolute value could be probably attributed to the removal of amorphous regions with existing charge.

The samples were analyzed with XPS in order to evaluate the presence of carboxylate and sulphate groups on the surface. The results are presented in Table 1. Presence of carboxylate groups was observed in all the samples. There are previous reports [47] that chemical bleaching leads to introduction of carboxylate groups on cellulose surface. The highest carboxylate content was observed for NcCA sample that was obtained from chemical process (*Route 1*) and had been subjected to four bleaching steps, compared to other samples (*Route 2* and *3*) that were treated with one single bleaching step and displayed a lower amount of carboxylate groups. Pretreatment with enzyme cocktail B that contained the PclPMO9D (*Route 3*) resulted in nano-scale cellulose with higher carboxylate content (sample NcE₁E) than the cocktail A without LPMO (*Route 2*, Sample NcEE), as expected by the C1-activity of the enzyme. Both *Routes 2b* and *3b* resulted in samples without sulphate groups, which were more susceptible to the post-treatment with LPMOs, as shown below, regarding the increase of the carboxylate content, compared to the samples obtained from the chemical process (*Route 1*). Regarding the presence of sulphate groups, all samples obtained after acid hydrolysis showed a relatively high amount of these surface groups. It was also observed, as expected, that replacing acid hydrolysis with endoglucanase-catalyzed treatment resulted in samples without sulphate groups (NcEE and NcE₁E).

Regarding the thermostability of the nano-scale cellulose, the thermal properties of the isolated samples is presented in Fig. 4. Both onset and peak degradation temperature values of the NcCA sample prepared from *Route 1* are very similar to those previously isolated from tunicate biomass by similar processes [5] and they also show typical characteristics to others reported in the literature [14,48]. Comparing the thermal stability of NcCA with that of samples from *Routes 2* and *3*, it can be observed that, as expected, the thermal stability of NcCA is the lowest; this can be attributed to the presence of sulphonate half-ester groups that promote charring of the cellulose [49], rendering it more sensitive to thermal degradation. In fact, the results show a trend that is directly proportional to the atomic percentage of sulphate groups detected by XPS (Table 1). Apart from the presence of sulphonate half-ester groups, it has been reported that the thermal stability of nanocellulose is also affected by bleaching [49], which may be a possible explanation for the higher stability of NcEA and NcE₁A samples compared to the NcCA. Samples NcEE and NcE₁E that have been prepared from enzymatic routes in the absence of acid hydrolysis (*Routes 2b* and *3b*) exhibit higher stability than that of their counterparts from enzymatic/acid routes (*Routes 2a* and *3a*), possibly due to the absence of sulphate groups. The thermal properties of NcEE and NcE₁E exhibit

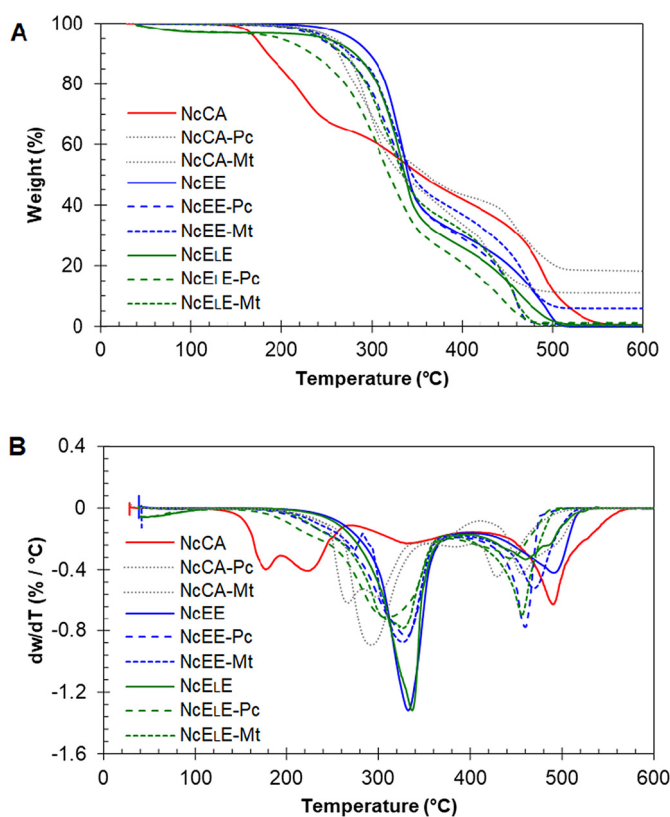


Fig. 4. (A) Thermogravimetric analysis (TGA) and (B) differential thermogravimetry (DTG) curves of isolated nano-scale cellulose prior and after post-treatment with different LPMOs.

only slight differences, which indicates that the addition of PclPMO in the enzymatic cocktail during pre-treatment (*Route 3*) has practically no effect on the thermostability of the samples, which has also been reported in the work of Hu et al., 2018 [27].

3.4. Post-treatment of isolated nano-scale cellulose with different LPMOs

Three samples, namely NcCA, NcEE and NcE₁E were chosen to further evaluate the effect of LPMO post-treatment by using two enzymes with different regioselectivity. In addition to PclPMO9D that oxidizes C1 carbon with an already proved effect in introducing carboxylate groups, MtlPMO9H that has a double C1/C4-oxidative action was chosen. In our previous work, MtlPMO9H has been shown to be an efficient oxidative biocatalyst that promoted the production of negatively charged thin cellulose nanocrystals from organosolv pretreated tunicate biomass [5].

First, to confirm that both LPMOs were active on the isolated nanocellulose samples, the soluble fraction after LPMO treatment was analyzed with HPAEC-PAD for the presence of oxidized sugars (Supplementary material, Fig. S2). PclPMO9D was active on all three samples, showing the highest activity on NcE₁E sample and the lowest on NcCA. MtlPMO9H also showed activity on all three samples with no significant differences, releasing C1, C4 and C1/C4-double oxidized products. Overall, the sample from chemical process (*Route 1*, NcCA) showed the lowest amount of released soluble products after the post-treatment with LPMOs, which can be possibly attributed to the presence of high amount of carboxylate and sulphate groups that might hamper the activity of the enzymes. However, these measurements provide only an indication of the LPMO activity based on oxidized sugars that are present in the reaction medium, therefore they cannot be directly correlated to the activity of the enzyme on the insoluble fraction, namely the nanocellulose. Surface analysis of the nano-scale product,

as described below, is more appropriate to evaluate the effect of each LPMO.

The morphology of the samples after the post-treatment is depicted at Fig. 2. It is obvious that in all cases, the activity of the enzymes led to thinner and well-dispersed nano-scale cellulose crystals and fibers, with relatively good colloidal stability in the aqueous solution, especially for NcCA and NcE₁E, as verified by the zeta-potential values described at Fig. 3. Since C1-acting LPMOs create nicks on the surface of the cellulose crystalline areas while introducing carboxylate groups [33], it is expected that their activity promotes defibrillation. As a result, there is a decrease in the width of nanocellulose elements, which is more profound in case of MtLPMO9H; the activity of this LPMO yields very thin structures comprised of few elementary fibrils, which is in accordance with results from treatment of tunicate-derived nanocellulose [5]. As shown by the AFM analysis at Fig. 2, the length of the fibrils is high, indicating that the produced nano-scale cellulose has a high aspect ratio. Nanocellulose with a high aspect ratio, especially when it is sulphur-free as in the case of this work, meets the requirements for numerous applications [1].

The surface groups of the samples were identified with XPS and the results are presented in Table 1. Regarding the LPMO regioselectivity and the introduction of carboxylate groups, PcLPMO9D was shown as a strong candidate in enhancing the –COOH groups, as expected. Treatment with PcLPMO9D increased the carboxylate content from 0.59 to 1.26 for NcEE and 0.79 to 1.55 for NcE₁E, but not for sample NcCA, where the enzyme indeed showed the lower activity, as also proved by the release of lower amount of soluble products. The amount of sulphate groups was reduced after LPMO treatment, which might be attributed to the oxidative cleavage activity of the enzymes. The above observation leads to the assumption that during LPMO treatment, there is a competition between sulphate and carboxylate groups for substitution at the primary alcohol. Interestingly, there is a recent study reporting a reduction in sulphur content of nanocrystals isolated after sulphuric acid treatment that were subsequently treated with TEMPO, which confirms a similar behavior to what was observed in our study [50]. During MtLPMO9H post-treatment, a slight reduction in carboxylate group was observed for NcCA and NcE₁E.

Regarding the zeta-potential values that are shown in Fig. 3, the standard deviation of the measurements indicates that there are slight differences after the activity of LPMOs, even in case of PcLPMO9D that has a strong oxidative effect on the substrate according to the XPS data. In case of NcCA also the removal of charged sulphate groups after the LPMO post-treatment, as verified by XPS analysis and as explained above, is expected [10,46]. In case of NcEE, no significant differences are observed despite the increase of the COOH groups from both enzymes. One hypothesis for this paradox could be that the LPMO activity facilitates cellulose defibrillation [33,34] and leads the exposure of new unmodified surfaces. These new inner portions of the cellulose particles may have different surface chemistry than those previously exposed, which affects the zeta-potential value.

Regarding the thermal stability properties of the samples, the results shown on Fig. 4 indicate a decreased thermostability of all three samples (NcCA, NcEE and NcE₁E) after post-treatment with both LPMOs, and this trend is more profound in case of MtLPMO9H. One could expect that the higher amount of carboxylate groups in samples post-treated with PcLPMO9D would possibly lead to lower thermostability, however the opposite is observed and the presence of carboxylate groups seems not to have a significant impact. The results may be related to the disruption of the fibers, as also reflected by the reduction of the fiber width (Fig. 2), leading to reduction of the overall crystallinity of the sample. The changes in crystallinity have a greater effect on the thermal properties of the material, as previously reported [27].

In general, it was observed that the LPMO post-treatment step leads to modification of the nano-scale cellulose in terms of defibrillation and enhanced carboxyl content for the non-sulfated samples (samples NcEE and NcE₁E). However, the distinct behavior of the two enzymes on sulphated CNCs (sample NcCA) requires further attention, as none of

the LPMOs could enhance the carboxyl content of chemically obtained NcCA, but both LPMOs significantly changed the morphology in terms of reduced particle width. The defibrillation ability of a C1-active LPMO on sulphated nanocrystals and release of soluble sugars has been reported previously [51], but its correlation to introduction of carboxyl groups is not well explored. Another scenario is that, LPMOs were in fact active on NcCA, resulting in thinner fibers with reduced sulphate content as observed from XPS (due to the removal of those regions by enzyme action), and might have also introduced carboxyl groups with C1 specificity as expected. However, the enzyme action might also have resulted in the removal of already existed carboxyl groups (introduced from bleaching stage). Since NcCA had high amount of pre-existed unspecific carboxyl groups than NcEE and NcE₁E, the new introduction of C1 specific carboxyl groups by LPMOs was perhaps lower or equal to the amount of carboxyl groups the substrate lost due to enzyme action, resulting in a no net increase. As XPS is an unspecific detection method for the location specificity of carboxyl groups, this scenario could not be evaluated with the obtained data.

4. Conclusions

Different monoenzymes with specified cellulolytic, hemicellulolytic and oxidative activities were successfully used for the isolation of sulphur-free nanocellulose from birch. Our results demonstrate that a combination of organosolv pretreatment in the absence of any acid, followed by two enzymatic treatment steps, and final refining with post-treatment modification with the C1-specific PcLPMO9D is the best strategy to produce nano-scale cellulose with high carboxylate content and improved thermal properties. The proposed process is novel from not only the perspective of organosolv pretreatment and valorization of forest biomass, but also because individual enzymes were employed for targeting the removal of cellulose amorphous areas, instead of commercial cellulase cocktails with a broad activity.

CRedit authorship contribution statement

Madhu Nair Muraleedharan: Conceptualization, Investigation, Methodology, Validation, Writing – original draft. **Anthi Karnaouri:** Conceptualization, Methodology, Validation, Writing – original draft, Visualization. **Majka Piatkova:** Methodology, Investigation, Validation. **Maria-Ximena Ruiz-Caldas:** Investigation, Validation. **Leonidas Matsakas:** Investigation, Validation, Visualization. **Bing Liu:** Investigation, Validation. **Ulrika Rova:** Methodology, Visualization. **Paul Christakopoulos:** Resources, Writing – review & editing, Supervision. **Aji P. Mathew:** Conceptualization, Validation, Resources, Writing – review & editing, Supervision.

Declaration of competing interest

Authors declare that they have no known competing financial interests or personal relationships that could have appeared to influence the work reported in this paper.

Acknowledgements

Not applicable.

Appendix A. Supplementary data

Supplementary data to this article can be found online at <https://doi.org/10.1016/j.ijbiomac.2021.04.136>.

References

- [1] D. Trache, A.F. Tarchoun, M. Derradji, T.S. Hamidon, N. Masruchin, N. Brosse, et al., Nanocellulose: from fundamentals to advanced applications, *Front. Chem.* 8 (2020) 392.

- [2] D. Klemm, F. Kramer, S. Moritz, T. Lindström, M. Ankerfors, D. Gray, et al., Nanocelluloses: a new family of nature-based materials, *Angew. Chem. Int. Ed.* 50 (2011) 5438.
- [3] O. Nechyporchuk, M.N. Belgacem, J. Bras, Production of cellulose nanofibrils: a review of recent advances, *Ind. Crop. Prod.* 93 (2016) 2–25.
- [4] L. Brinchi, F. Cotana, E. Fortunati, J.M. Kenny, Production of nanocrystalline cellulose from lignocellulosic biomass: technology and applications, *Carbohydr. Polym.* 94 (1) (2013) 154–169.
- [5] A. Karnaouri, B. Jalvo, P. Moritz, L. Matsakas, U. Rova, O. Höft, et al., Lytic polysaccharide monoxygenase-assisted preparation of oxidized-cellulose nanocrystals with a high carboxyl content from the tunic of marine invertebrate *Ciona intestinalis*, *ACS Sustain. Chem. Eng.* 8 (50) (2020) 18400–18412.
- [6] P. Squinca, S. Bilatto, A.C. Badino, C.S. Farinas, Nanocellulose production in future biorefineries: an integrated approach using tailor-made enzymes, *ACS Sustain. Chem. Eng.* 8 (5) (2020) 2277–2286.
- [7] M. Jonoobi, A.P. Mathew, K. Oksman, in: K. Oksman, A.P. Mathew, A. Bismarck, O. Rojas, M. Sain (Eds.), *Ch 3. Handbook of Green Materials 1. Bionanomaterials: Separation Processes, Characterisation and Properties*, World Scientific Publishing Co 2014, pp. 19–32.
- [8] A. García, A. Gandini, J. Labidi, N. Belgacem, J. Bras, Industrial and crop wastes: a new source for nanocellulose biorefinery, *Ind. Crop. Prod.* 93 (2016) 26–38.
- [9] S. Panthapulakkal, M. Sain, Preparation and characterization of cellulose nanofibril films from wood fibre and their thermoplastic polycarbonate composites, *Int. J. Polym. Sci.* 2012 (2012), 381342.
- [10] D. Bondeson, A. Mathew, K. Oksman, Optimization of the isolation of nanocrystals from microcrystalline cellulose by acid hydrolysis, *Cellulose* 13 (2) (2006) 171.
- [11] A. Dufresne, *Nanocellulose: From Nature to High Performance Tailored Materials*, Walter de Gruyter GmbH & Co KG, 2017.
- [12] A. Isogai, T. Saito, H. Fukuzumi, TEMPO-oxidized cellulose nanofibers, *Nanoscale* 3 (1) (2011) 71–85.
- [13] L. Wågberg, G. Decher, M. Norgren, T. Lindström, M. Ankerfors, K. Axnäs, The build-up of polyelectrolyte multilayers of microfibrillated cellulose and cationic polyelectrolytes, *Langmuir* 24 (3) (2008) 784–795.
- [14] M. Rosa, E.S. Medeiros, J.A. Malmonge, K.S. Gregorski, D.F. Wood, L.H.C. Mattoso, et al., Cellulose nanowhiskers from coconut husk fibers: effect of preparation conditions on their thermal and morphological behavior, *Carbohydr. Polym.* 81 (1) (2010) 83–92.
- [15] Z. Hanif, F.R. Ahmed, S.W. Shin, Y.K. Kim, S.H. Um, Size- and dose-dependent toxicity of cellulose nanocrystals (CNC) on human fibroblasts and colon adenocarcinoma, *Colloids Surf. B: Biointerfaces* 119 (2014) 162–165.
- [16] H. Xie, H. Du, X. Yang, C. Si, Recent strategies in preparation of cellulose nanocrystals and cellulose nanofibrils derived from raw cellulose materials, *Int. J. Polym. Sci.* 2018 (2018), 7923068.
- [17] O. Rosales-Calderon, V. Arantes, A review on commercial-scale high-value products that can be produced alongside cellulosic ethanol, *Biotechnol. Biofuels* 12 (1) (2019), 240.
- [18] S. Jayasekara, R. Ratnayake, Microbial cellulases: an overview and applications, *Cellulose* (2019) 22.
- [19] R.S. Teixeira, A.S. da Silva, J.H. Jang, H.W. Kim, K. Ishikawa, T. Endo, et al., Combining biomass wet disk milling and endoglucanase/ β -glucosidase hydrolysis for the production of cellulose nanocrystals, *Carbohydr. Polym.* 128 (2015) 75–81.
- [20] Y. Xu, J. Salmi, E. Kloser, F. Perrin, S. Grosse, J. Denault, P. Lau, Feasibility of nanocrystalline cellulose production by endoglucanase treatment of natural bast fibers, *Ind. Crop. Prod.* 51 (2013) 381–384.
- [21] G.A. Siqueira, I. Dias, V. Arantes, Exploring the action of endoglucanases on bleached eucalyptus kraft pulp as potential catalyst for isolation of cellulose nanocrystals, *Int. J. Biol. Macromol.* 133 (2019) 1249–1259.
- [22] D. Beyene, M. Chae, J. Dai, C. Danumah, F. Tosto, A.G. Demesa, et al., Characterization of cellulase-treated fibers and resulting cellulose nanocrystals generated through acid hydrolysis, *Materials* 11 (8) (2018) 1272.
- [23] F. Beltramino, M. Blanca Roncero, T. Vidal, C. Valls, A novel enzymatic approach to nanocrystalline cellulose preparation, *Carbohydr. Polym.* 189 (2018) 39–47.
- [24] Z. Yuan, W. Wei, Y. Wen, Improving the production of nanofibrillated cellulose from bamboo pulp by the combined cellulase and refining treatment, *J. Chem. Technol. Biotechnol.* 94 (2019) 2178–2186.
- [25] B.R. Rossi, V.O.A. Pellegrini, A.A. Cortez, E.M.S. Chiromito, A.J.F. Carvalho, L.O. Pinto, et al., Cellulose nanofibers production using a set of recombinant enzymes, *Carbohydr. Polym.* 256 (2021) 117510.
- [26] S. Koskela, S. Wang, D. Xu, X. Yang, X. Li, L.A. Berglund, et al., Lytic polysaccharide monoxygenase (LPMO) mediated production of ultra-fine cellulose nanofibres from delignified softwood fibres, *Green Chem.* 21 (21) (2019) 5924–5933.
- [27] J. Hu, D. Tian, S. Renneckar, J.N. Saddler, Enzyme mediated nanofibrillation of cellulose by the synergistic actions of an endoglucanase, lytic polysaccharide monoxygenase (LPMO) and xylanase, *Sci. Rep.* 8 (1) (2018), 3195.
- [28] C. Valls, F. Pastor, M.B. Roncero, T. Vidal, P. Diaz, J. Martínez, et al., Assessing the enzymatic effects of cellulases and LPMO in improving mechanical fibrillation of cotton linters, *Biotechnol. Biofuels* 12 (2019) 161.
- [29] H. Zhou, F.S. John, J.J.C. Zhu, Xylanase Pretreatment of Wood Fibers for Producing Cellulose Nanofibrils: A Comparison of Different Enzyme Preparations, 26(1), 2019 543–555.
- [30] V.G.H. Eijssink, D. Petrovic, Z. Forsberg, S. Mekasha, Å.K. Röhr, A. Várnai, et al., On the functional characterization of lytic polysaccharide monoxygenases (LPMOs), *Biotechnol. Biofuels* 12 (2019) 58.
- [31] A. Karnaouri, M.N. Muraleedharan, M. Dimarogona, E. Topakas, U. Rova, M. Sandgren, et al., Recombinant expression of thermostable processive MtEG5 endoglucanase and its synergism with MtLPMO from *Myceliophthora thermophila* during the hydrolysis of lignocellulosic substrates, *Biotechnol. Biofuels* 10 (2017) 126.
- [32] B. Liu, S. Krishnaswamyreddy, M.N. Muraleedharan, Å. Olson, A. Broberg, J. Ståhlberg, et al., Side-by-side biochemical comparison of two lytic polysaccharide monoxygenases from the white-rot fungus *Heterobasidion irregulare* on their activity against crystalline cellulose and glucomannan, *PLoS One* 13 (9) (2018), e0203430.
- [33] C. Moreau, S. Tapin-Lingua, S. Grisel, I. Gimbert, S. Le Gall, V. Meyer, et al., Lytic polysaccharide monoxygenases (LPMOs) facilitate cellulose nanofibrils production, *Biotechnol. Biofuels* 12 (2019), 156.
- [34] A. Villares, C. Moreau, C. Bennati-Granier, S. Garajova, L. Foucat, X. Falourd, et al., Lytic polysaccharide monoxygenases disrupt the cellulose fibers structure, *Sci. Rep.* 7 (2017), 40262.
- [35] S.V. Valenzuela, C. Valls, V. Schink, D. Sánchez, M.B. Roncero, P. Diaz, et al., Differential activity of lytic polysaccharide monoxygenases on celluloses of different crystallinity. Effectiveness in the sustainable production of cellulose nanofibrils, *Carbohydr. Polym.* 207 (2019) 59–67.
- [36] B. Westereng, T. Ishida, G. Vaaje-Kolstad, M. Wu, V.G. Eijsink, K. Igarashi, et al., The putative endoglucanase PcGH61D from *Phanerochaete chrysosporium* is a metal-dependent oxidative enzyme that cleaves cellulose, *PLoS One* 6 (11) (2011).
- [37] K.G. Kalogiannis, L. Matsakas, J. Aspden, A.A. Lappas, U. Rova, P. Christakopoulos, Acid-assisted organosolv delignification of beechwood and pulp conversion towards high concentrated cellulosic ethanol via high gravity enzymatic hydrolysis and fermentation, *Molecules* 23 (7) (2018) 1647.
- [38] J.B. Sluiter, R.O. Ruiz, C.J. Scarlata, A.D. Sluiter, D.W. Templeton, Compositional analysis of lignocellulosic feedstocks. 1. Review and description of methods, *J. Agric. Food Chem.* 58 (16) (2010) 9043–9053.
- [39] M. Dimarogona, E. Topakas, L. Olsson, P. Christakopoulos, Lignin boosts the cellulase performance of a GH-61 enzyme from *Sporotrichum thermophile*, *Bioresour. Technol.* 110 (2012) 480–487.
- [40] B. Liu, Å. Olson, M. Wu, A. Broberg, M. Sandgren, Biochemical studies of two lytic polysaccharide monoxygenases from the white-rot fungus *Heterobasidion irregulare* and their roles in lignocellulose degradation, *PLoS One* 12 (12) (2017), e0189479.
- [41] A.C. Rodrigues, M.Ø. Haven, J. Lindedam, C. Felby, M. Gama, Celluclast and Cellic® Ctec2: Saccharification/fermentation of wheat straw, solid-liquid partition and potential of enzyme recycling by alkaline washing, *Enzym. Microb. Technol.* 79–80 (2015) 70–77.
- [42] A. Karnaouri, L. Matsakas, S. Bühler, M.N. Muraleedharan, P. Christakopoulos, U. Rova, Tailoring Celluclast® Cocktail's performance towards the production of prebiotic cello-oligosaccharides from waste forest biomass, *Catalysts* 9 (2019) 897.
- [43] G. Cheng, S. Datta, Z. Liu, C. Wang, J.K. Murton, P.A. Brown, et al., Interactions of endoglucanases with amorphous cellulose films resolved by neutron reflectometry and quartz crystal microbalance with dissipation monitoring, *Langmuir* 28 (22) (2012) 8348–8358.
- [44] J.M. Yarbrough, R. Zhang, A. Mittal, T. Vander Wall, Y.J. Bomble, S.R. Decker, et al., Multifunctional cellulolytic enzymes outperform processive fungal cellulases for co-production of nanocellulose and biofuels, *ACS Nano* 11 (3) (2017) 3101–3109.
- [45] Q. Lin, Y. Yan, X. Liu, B. He, X. Wang, X. Wang, et al., Production of xylooligosaccharide, nanolignin, and nanocellulose through a fractionation strategy of corncob for biomass valorization, *Ind. Eng. Chem. Res.* 59 (39) (2020) 17429–17439.
- [46] L.J. Johnston, Z.J. Jakubek, S. Beck, J. Araki, E.D. Cranston, C. Danumah, et al., Determination of sulfur and sulfate half-ester content in cellulose nanocrystals: an interlaboratory comparison, *Metrologia* 55 (2018) 872.
- [47] Z. Dang, T. Elder, A.J. Ragauskas, Alkaline peroxide treatment of ECF bleached softwood kraft pulps. Part 1. Characterizing the effect of alkaline peroxide treatment on carboxyl groups of fibers, *Holzforchung* 61 (4) (2007) 445–450.
- [48] M. Roman, W.T. Winter, Effect of sulfate groups from sulfuric acid hydrolysis on the thermal degradation behavior of bacterial cellulose, *Biomacromolecules* 5 (2004) 1671–1677.
- [49] M. Jonoobi, J. Harun, A. Shakeri, M. Misra, Chemical composition, crystallinity, and thermal degradation of bleached and unbleached kenaf bast (*Hibiscus cannabinus*) pulp and nanofibers, *BioResources* 4 (2009) 626–639.
- [50] J.K. Hong, S.L. Cooke, A.R. Whittington, M. Roman, Bioactive cellulose nanocrystal-poly(ϵ -caprolactone) nanocomposites for bone tissue engineering applications, *Front. Bioeng. Biotechnol.* 9 (2021), 605924.
- [51] M. Eibinger, J. Sattelkow, T. Ganner, H. Plank, B. Nidetzky, Single-molecule study of oxidative enzymatic deconstruction of cellulose, *Nat. Commun.* 8 (2017) 894.